AFORS-HET, A NUMERICAL PC-PROGRAM FOR SIMULATION OF (THIN FILM) HETEROJUNCTION SOLAR CELLS, VERSION 2.0 (OPEN-SOURCE ON DEMAND), TO BE DISTRIBUTED FOR PUBLIC USE

R. Stangl, M. Kriegel, M. Schmidt

Hahn-Meitner-Institut Berlin (HMI), Abteilung Silizium Photovoltaik, Kekulé-Str. 5, D-12489 Berlin, Germany
*Corresponding author: e-mail: stangl@hmi.de, tel: +49/30/8062-1312, fax: +49/30/8062-1333

ABSTRACT: We offer the (open-source on demand) Version 2.0 of AFORS-HET, a numerical computer simulation program for modeling (thin film) heterojunction solar cells. This version now allows time dependent (transient state) calculations. The time response of the system due to a sudden change of the external cell voltage/current and or illumination can be calculated. It will be distributed free of charge on CD-ROM at the conference site and can also be downloaded via internet: www.hmi.de/bereiche/SE/SE1/projects/aSicSi/AFORS-HET (note: this link is case sensitive).

Keywords: Simulation, Heterojunction, Experimental Methods, Thin Film

1 INTRODUCTION

In order to investigate (thin film) heterojunction solar cells, a variety of different experimental methods are used, ranging from standard solar cell characterization techniques like current-voltage or quantum efficiency to more advanced characterization techniques like for example surface photovoltage, photo- and electro-luminescence, capacitance/impedance, intensity modulated photocurrent spectroscopy or electrically detected magnetic resonance.

In order to support the interpretation of such measurements, we developed a numerical simulation tool (**AFORS-HET**, **a**utomat **for** **s**imulation of **het**ero-structures). AFORS-HET not only simulates (thin film) heterojunction solar cells, but also the observable of the corresponding measurement techniques. A user-friendly graphical interface allows the visualisation, storage and comparison of all simulation data. Furthermore, arbitrary parameter variations and parameter fits to the corresponding measurements can be performed. Different numerical modules permit to treat different experimental situations, as for example a metal/semiconductor or a metal/insulator/semiconductor front contact, that can be chosen freely.

Up to now, we used AFORS-HET mainly to simulate amorphous/crystalline silicon heterojunction solar cells of the structure TCO/a-Si:H(n)/a-Si:H(i)/c-Si(p)/a-Si:H(p^+)/Al, where ultra-thin layers (5 nm) of amorphous hydrogenated silicon are deposited on top of a thick (300 µm) crystalline c-Si(p) wafer. Experimentally, we realized efficiencies larger than 18% [1].

2 MODELLING CAPABILITIES

An arbitrary sequence of semiconducting layers can be modelled, specifying the corresponding layer and interface properties, i.e. the defect distribution of states (DOS). Using Shockley-Read-Hall recombination statistics, the one-dimensional semiconductor equations are solved (1) for thermodynamic equilibrium, (2) for steady-state conditions under an external applied voltage or current and/or illumination, (3) for small additional sinusoidal modulations of the external applied voltage/illumination, (4) for transient conditions, due to sudden changes of the external applied voltage or current and/or illumination. Thus, the internal cell characteristics, such as band diagrams, local generation and recombination rates, local cell currents, carrier densities and phase shifts can be calculated. Furthermore, a variety of characterisation methods can be simulated, i.e.: current-voltage (I-V), internal and external quantum efficiency (IQE, EQE), intensity and voltage dependent surface photovoltage (SPV), photo- and electroluminescence (PL, EL), impedance spectroscopy (IMP), capacitance-frequency (C-f), capacitance-voltage (C-V), capacitance-temperature (C-T) and electrical detected magnetic resonance (EDMR). The graphical interface enables the user to perform arbitrary parameter variations and parameter-fits to measurements.

Version 2.0 is modulized in a form, that new measurement methods and new numerical modules can be implemented by external users (open-source on demand). So far, the following numerical modules have been developed: (a) metal/semiconductor Schottky- or metal/insulator/semiconductor MIS- front contact, (b) drift diffusion or thermionic emission transport across the semiconductor/semiconductor heterojunction interface, (c) optical layers (coherent or incoherent multiple reflection) in order to calculate the generation rate.

3 NUMERICAL INFORMATION

In the following, only the modifications of the differential equations and corresponding boundary conditions are stated, which are solved by AFORS-HET within the new transient calculation mode. For general information, see [2,3].

AFORS-HET numerically solves the one-dimensional semiconductor equations with appropriate boundary conditions. The set of coupled partial differential equations is transformed into a set of nonlinear algebraic equations by the method of finite differences. Up to now, the grid on which the equations are solved is fixed at the beginning of the calculation (fixed x-discretization, non-adaptive meshing), but can be modified by the user, if needed. At each grid point i, the free electron density n_i, the free hole density p_i and the cell potential φ_i are used as independent variables. All other variables in the discretized differential equations and boundary conditions are expressed in such

a way that they only depend on these independent variables. The resulting nonlinear equations are solved using the Newton-Raphson iteration scheme.

With the ability to calculate internal cell characteristics under various specified external boundary conditions, measurement methods can be defined by a specific variation of the external boundary conditions and some additional post-processing data analysis.

3.1 Bulk

Poisson's equation and the transport equation for electrons and holes are solved in one dimension x for a given time point t:

$$\frac{\varepsilon_0 \varepsilon_r}{q}\frac{\partial^2 \varphi(x,t)}{\partial x^2} = p(x,t) - n(x,t) + N_D - N_A + \rho_t(x,t)$$

$$-\frac{1}{q}\frac{\partial j_n(x,t)}{\partial x} = G_n(x,t) - R_n(x,t) \; - \frac{\partial}{\partial t} n(x,t)$$

$$\frac{1}{q}\frac{\partial j_p(x,t)}{\partial x} = G_p(x,t) - R_p(x,t) \; - \frac{\partial}{\partial t} p(x,t)$$

The electron density n, the hole density p and the electric potential φ are the independent variables for which the system of differential equations is solved (q: electron charge, ε_0, ε_r: absolute/relative dielectric constant, $j_{n/p}$: electron/hole currents, G_n, G_p: electron/hole generation rates, R_n, R_p: net electron/hole recombination rates, $N_{D/A}$: completely ionized donor/acceptor concentrations). The trapped charge stored in the defects, $\rho_t = \rho_p - \rho_n$, is described by a distribution function f_t, specifying the probability that defects with defect density N_t at the energy position E within the bandgap are occupied with electrons:

acceptor-type defect:

$$\rho_n(x,t) = \sum_{\text{defects}} \int dE \; f_t(E,x,t)\, N_t(E)$$

donator-type defect:

$$\rho_p(x,t) = \sum_{defects} \int dE \; \left(1 - f_t(E,x,t)\right) N_t(E)$$

3.1.1 Generation

There are no changes compared to the steady-state calculation mode, compare [2].

3.1.2 Recombination

Recombination from the conduction band into the valence band may occur directly (band to band recombination, Auger recombination) and via trap states (Shockley-Read-Hall recombination, SHR). An arbitrary number of defects distributed arbitrarily within the bandgap of the semiconductor layers can be specified. SHR recombination requires to specify the energetic distribution of the defect density $N_t(E)$ of each defect and its electron/hole capture coefficients $c_{n,p} = v_{n,p}\sigma_{n,p}$ ($v_{n,p}$: thermal velocity, $\sigma_{n,p}$: capture cross section). The emission rates $e_{n,p}$ can then be specified, see [2], and the net SRH recombination rate R_n^{SRH}, R_p^{SRH} (>0: recombination, <0: generation) due to the defects is

$$R_n^{SRH}(x,t) = \sum_{defects} \int dE \left\{ c_n n(x) N_t(E)\left(1 - f_t(E,x,t)\right) - e_n(x) N_t(E) f_t(E,x,t) \right\}$$

$$R_p^{SRH}(x,t) = \sum_{defects} \int dE \left\{ c_p p(x) N_t(E) f_t(E,x,t) - e_p(x) N_t(E)\left(1 - f_t(E,x,t)\right) \right\}$$

3.1.3 Defect distribution function

In case of using the equilibrium (EQ), the steady-state (DC) or the small additional sinusoidal modulations (AC) calculation mode the SHR distribution function $f_t(E,x,t)$ describing the defect state electron occupation probability can be explicitely stated. In case of using the transient calculation mode, the SHR distribution function for each defect will be implicitely determined. The super-bandgap generation rate due to photon absorption is equal for electrons and holes: $G_p(x,t) = G_n(x,t)$. This is also true for the direct electron/hole recombination. Thus, the local change of the trapped charge stored in the defects is determined by the difference between the net SHR local hole and electron recombination rate:

$$\frac{d}{dt}\rho_t(x,t) = R_p^{SHR}(x,t) - R_n^{SHR}(x,t)$$

This defines differential equations for each SHR defect distribution function $f_t(E,x,t)$:

$$\frac{d}{dt} f_t(E,x,t) = \left(c_n n(x,t) + e_p(x)\right)\left(1 - f_t(E,x,t)\right) - \left(c_p p(x,t) + e_n(x)\right) f_t(E,x,t) \qquad (*)$$

In case of using the EQ or DC calculation mode, the time derivative vanishes, and explicit expressions for $f_t(E,x,t)$ can be derived. This is also possible, if one assumes small additional sinusoidal modulations (AC mode). The corresponding formulas are cited in [2]. In case of using the transient calculation mode, there is now an additional differential equation for each defect, specifying the transient SHR-defect distribution function $f_t(E,x,t)$, which has to be solved.

In general, a stable, fully implicit calculation scheme should be used (assuming the right hand side of equation (*) to occur at the time point t_{i+1} when performing the time discretisation). This will enhance the amount of discretised equations, which have to be solved simultaneously. However, so far, an explicit calculation scheme is used (assuming the right hand side of equation (*) to occur at the time point t_i when performing the time discretisation). Thus, an explicit expression for the distribution functions can be derived:

$$f_{t_{i+1}} = f_{t_i} + (t_{i+1} - t_i)\left\{\left(c_n n_{t_i} + e_p\right)\left(1 - f_{t_i}\right) - \left(c_p p_{t_i} + e_n\right) f_{t_i}\right\}$$

Therefore, still only 3 discretised equations have to be solved simultaneously (solving for $n_{t_{i+1}}, p_{t_{i+1}}, \varphi_{t_{i+1}}$). However, the time discretisation has to be chosen properly by the user in order to reach convergence.

The DC steady state solution is used as a starting solution, before some sudden changes of the applied external cell voltage/current and/or illumination occur. Using the explicit iteration scheme sketched above, the electron/hole density $n_{t_{i+1}}(x)$, $p_{t_{i+1}}(x)$ and the potential $\varphi_{t_{i+1}}(x)$ is iteratively solved for each time step specified.

3.2 Interfaces

So far, the transient-state boundary conditions when specifying interfaces do not differ from the steady-state (DC) calculation mode. Note, however, that this is rigorously correct only if the drift-diffusion interface model is used. If using the thermionic emission interface model and performing a transient calculation, the steady-state distribution function of the interface defects should be modified in analogy to the procedure just mentioned above. However, this has not been implemented yet. Within version 2.0 of AFORS-HET, the steady-state distribution function is used instead as a first approximation.

3.3 Boundaries

There are no changes compared to the steady-state calculation mode, compare [2].

4 SELECTED RESULTS

In the following, we will demonstrate the capability of the program showing selected results on the simulation of TCO/a-Si:H(n)/c-Si(p)/Al silicon heterojunction solar cells. I.e., the influence of the a-Si:H/c-Si interface state density D_{it} on various characterization techniques is investigated. All figures shown are direct screenshots of the AFORS-HET program.

4.1 Input

Before calculation, an appropriate sequence of semiconducting layers and interfaces has to be defined. For the shown example, the corresponding semiconductor properties, namely the a-Si:H(n) thin film emitter and the c-Si(p) silicon wafer, must be stated. Additionally, the defect distribution of states (DOS) has to be specified for all layers and, if needed, for the interfaces. Furthermore the boundary contacts have to be specified: For the chosen example, the TCO layer is modeled as an optical layer (specifying the measured reflectivity and absorption). The TCO/a-Si:H contact is assumed to be depleted, whereas the measured barrier height of the contact serves as an input parameter. For the sake of simplicity, the c-Si(p)/Al contact is assumed to be flatband. Some screenshots of AFORS-HET input are presented in Fig. 1.

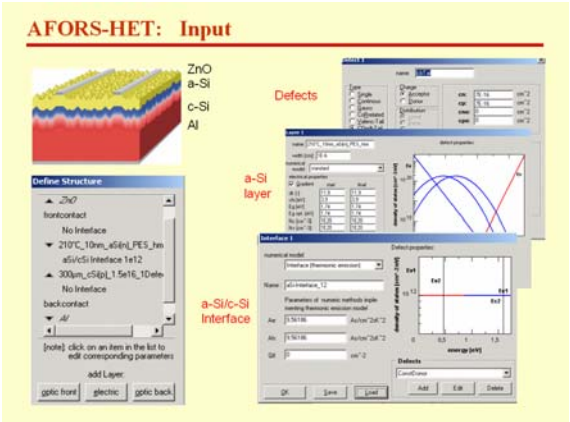

Figure 1: Typical input specification used for the simulation of TCO/a-Si:H(n)/c-Si(p)/Al silicon heterojunction solar cells. (left) layer sequence, (right) DOS of the a-Si:H(n) layer and the a-Si:H/c-Si interface.

4.2 internal cell characteristics: Band diagram

After the specification of the external cell parameters (temperature, illumination and external cell voltage or cell current through the boundary) the internal cell characteristics, such as band diagrams, local generation and recombination rates, local cell currents, carrier densities and phase shifts can be calculated.

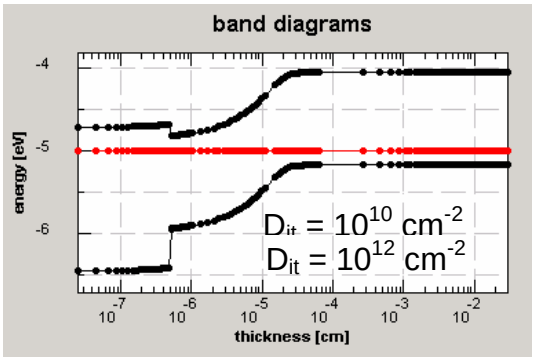

Figure 2: Band diagram for an a-Si:H(n)/c-Si(p) solar cell structure under equilibrium conditions, assuming different a-Si:H/c-Si interface state densities D_{it}.

If the a-Si:H/c-Si interface state density D_{it} is chosen to be in the range $10^{10}\text{cm}^{-2} \le D_{it} \le 10^{12}\text{cm}^{-2}$, it does not affect the equilibrium band bending, see Fig.2. However, it still cannot be neglected, as it significantly affects the open-circuit voltage of the solar cell, see Fig.3. Only for $D_{it} \le 10^{10}\text{cm}^{-2}$, the interface state density can be neglected.

4.3 DC-mode measurements: I-V, PL

Measurements can be simulated, just by varying external parameters like in a real experiment, and by performing some post-processing data analysis. So far, the following DC-mode measurements have been implemented: I-V, IQE, EQE, SPV, PL, EL and EDMR. Other measurement methods may be added or personally adopted by external users (open source on demand).

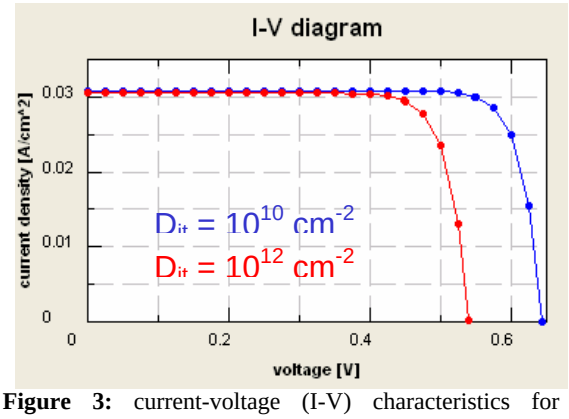

Figure 3: current-voltage (I-V) characteristics for a-Si:H(n)/c-Si(p) solar cell structures, assuming different a-Si/c-Si interface state densities D_{it}.

Varying the external cell voltage, the corresponding cell current can be calculated (I-V). The amount of emitted photons (PL) due to radiative band to band recombination can be calculated from the splitting of the quasi Fermi energies within the cell, using the generalized Planck equation [4].

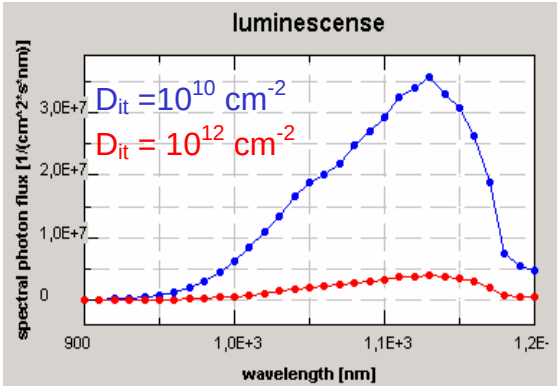

Figure 4: photoluminescence (PL) under open-circuit conditions, for a-Si:H(n)/c-Si(p) solar cell structures, assuming different a-Si/c-Si interface state densities D_{it}..

An interface state density of $D_{it}=10^{12}cm^{-2}$ reduces the open-circuit voltage of the solar cell by an amount larger than 100 mV, see Fig.3. Open-circuit photoluminescence proofs to be a fast and non-destructive characterization method, which is quite sensitive to D_{it} [5]. An increasing interface recombination due to a higher D_{it} quenches the radiative band to band recombination, see Fig.4.

4.4 AC-mode measurements: impedance

If one specifies a small additional sinusoidal modulation of the external cell voltage and/or illumination, AC-mode measurements can be performed. So far, the following AC-mode measurements have been implemented: IMP, C-f, C-V, C-T. Other measurement methods may be added or personally adopted by external users (open source on demand).

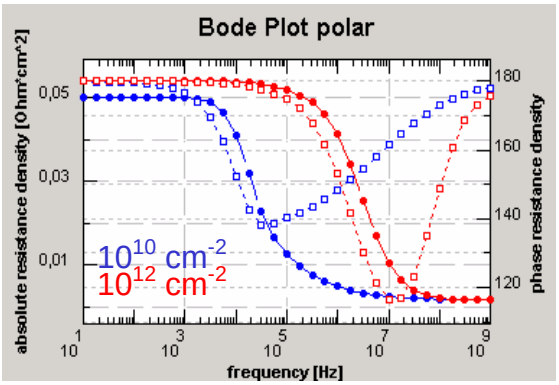

Figure 5: open-circuit impedance (IMP) for a-Si:H(n)/c-Si(p) solar cell structures, assuming different a-Si/c-Si interface state densities D_{it}.

The open-circuit impedance (IMP) is also very sensitive to the interface state density D_{it}. For higher Dit, the resonance frequency (maximum phase shift between AC cell voltage and AC cell current) is shifted towards higher frequencies, see Fig.5.

4.5 transient-mode calculations

If one specifies a sudden change of the external applied cell voltage or current and/or illumination, transient-mode calculations can be performed. That is, the time response of the system due to that sudden change will be calculated. So far, no transient-state measurements have been implemented. New measurement methods may be added by external users (open source on demand).

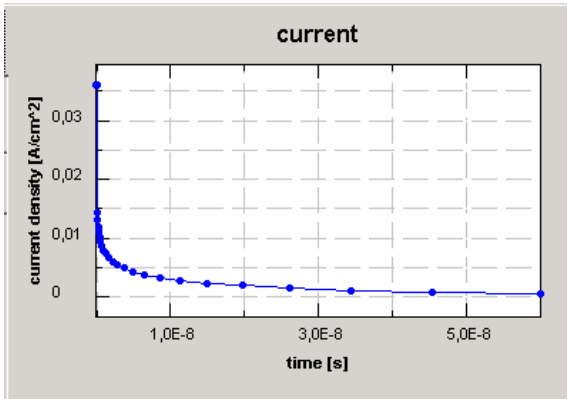

Figure 6: transient decay of the short circuit current, after the AM1.5 illumination has been switched off.

5 CONCLUSION

The new transient-mode capabilities of Version 2.0 of AFORS-HET have been quoted in terms of the underlying numerical computer modeling. Up to now, the program AFORS-HET has been mainly used in order (1) to evaluate maximum obtainable efficiencies for amorphous/crystalline solar cells, (2) to derive design criteria for these kind of solar cells, (3) to develop measurement methods for monitoring the a-Si:H/c-Si interface recombination, see [6-11]. AFORS-HET will be further developed (open-source on demand) and is available free of charge via internet.

6 ACKNOWLEDGEMENTS

The authors wish to acknowledge the financial support of the “Bundesministerium für Bildung und Forschung”, project Nr. 01SF0012.

7 REFERENCES

[1] Maydell, Nositschka, Windgassen, Rau, Schmidt, Henze, Borchert, Bauer, Tardon, Stiebig, Fahrner, Scherff, Schmidt, this conference, 2DO.3.6.
[2] Stangl, Froitzheim, Kriegel, Brammer, Kirste, Elstner, Stiebig, Schmidt, Fuhs, Version 1.1 of AFORS-HET, Proc. PVSEC-19, , Paris, France, June 2004, 1497.
[3] Stangl, Kriegel, Kirste, Schmidt, Fuhs, Proc. IEEE-31, Version 1.2 of AFORS-HET, Lake Buena Vista, USA, January 2005
[4] Würfel, The chemical potential of radiation, J. Phys. C 15, 1982, p.3967
[5] Schaffarzik, Stangl, Laades, Schubert, Schmidt, this conference, 2CV.5.34
[6] Stangl, Froitzheim, Fuhs, Proc. PV in Europe, Rome, Italy, October 2002, 123-126
[7] Stangl, Froitzheim, Schmidt, Fuhs, Proc. WCPEC-3, World Conf. PV En. Conv., Osaka, Japan, 2003, 4P-A8-45
[8] Schmidt, Korte, Kliefoth, Schoeppke, Stangl, Laades, Conrad, Brendel, Fuhs, Scherff, Fahrner, Proc. PVSEC-19, Paris, France, June 2004, 592
[9] Gudovskikh, Kleider, Stangl, Schmidt, Fuhs, Proc. PVSEC-19, Paris, France, June 2004, 697
[10] Stangl, Schaffarzik, Laades, Kliefoth, Schmidt, Fuhs, Proc. PVSEC-19, Paris, France, June 2004, 686
[11] Taguchi, Sakata, Yoshimine, Maruyama, Terakawa, Tanaka, Proc. IEEE-31, Lake Buena Vista, USA, Jan. 2005